Bioactive Materials 6 (2021) 4176–4185

Contents lists available at ScienceDirect

Bioactive Materials

journal homepage: www.sciencedirect.com/journal/bioactive-materials

Biodegradable magnesium pins enhanced the healing of transverse patellar fracture in rabbits

Dick Ho Kiu Chow [a,b], Jiali Wang [a,b], Peng Wan [c,d], Lizhen Zheng [a,b], Michael Tim Yun Ong [a], Le Huang [a,b], Wenxue Tong [a,b], Lili Tan [c], Ke Yang [c], Ling Qin [a,b,*]

[a] Musculoskeletal Research Laboratory, Department of Orthopaedics & Traumatology, The Chinese University of Hong Kong, Hong Kong SAR, China
[b] Innovative Orthopaedic Biomaterial and Drug Translational Research Laboratory, Li Ka Shing Institute of Health Sciences, The Chinese University of Hong Kong, Shatin, Hong Kong SAR, China
[c] Institute of Metal Research, Chinese Academy of Sciences, Shenyang, China
[d] School of Materials Science and Engineering, Dongguan University of Technology, Dongguan, China

ARTICLE INFO

Keywords:
Patellar fracture
Tension band wire
Biodegradable implant
Osteogenesis
Microindentation

ABSTRACT

Displaced fractures of patella often require open reduction surgery and internal fixation to restore the extensor continuity and articular congruity. Fracture fixation with biodegradable magnesium (Mg) pins enhanced fracture healing. We hypothesized that fixation with Mg pins and their degradation over time would enhance healing of patellar fracture radiologically, mechanically, and histologically. Transverse patellar fracture surgery was performed on thirty-two 18-weeks old female New Zealand White Rabbits. The fracture was fixed with a pin made of stainless steel or pure Mg, and a figure-of-eight stainless steel band wire. Samples were harvested at week 8 or 12, and assessed with microCT, tensile testing, microindentation, and histology. Microarchitectural analysis showed that Mg group showed 12% higher in the ratio of bone volume to tissue volume at week 8, and 38.4% higher of bone volume at week 12. Tensile testing showed that the failure load and stiffness of Mg group were 66.9% and 104% higher than the control group at week 8, respectively. At week 12, Mg group was 60.8% higher in ultimate strength than the control group. Microindentation showed that, compared to the Control group, Mg group showed 49.9% higher Vickers hardness and 31% higher elastic modulus at week 8 and 12, respectively. At week 12, the new bone of Mg group remodelled to laminar bone, but those of the control group remained woven bone-like. Fixation of transverse patellar fracture with Mg pins and its degradation enhanced new bone formation and mechanical properties of the repaired patella compared to the Control group.

1. Introduction

Patella is the largest sesamoid bone in the human body and plays a vital role in the extensor mechanism of the knee. Patellar fractures account for approximately 1% of all fractures with an overall incidence of 10.7 per 100,000 people per year, mostly seen in sports injuries and trauma [1–3]. Moreover, there is an increasing number of patellar fractures in the female and elderly population [4]. Since three-quarters of the posterior surface of the patella is covered by articular cartilage, most patellar fractures are intra-articular fractures that require anatomic reduction to restore joint congruency [4]. Transverse fracture of the patella is the most common and accounting for 50–80% of all patellar fractures [5]. For displaced fractures of patella, a surgical repair with open reduction and internal fixation is recommended. The most widely used internal fixation for patellar fracture is Kirschner wires (K-wires) with a tension band wire [2,6]. This technique aims to neutralize tension forces anteriorly produced by the extensor mechanism during knee flexion and converts them into stabilizing compressive forces at the articular surface of the patella [6]. Fixation of patellar fracture is important to allow early mobilization of the knee without detrimental displacement at the fracture site [7]. The modified tension band technique for the fixation of transverse patellar fracture has favorable clinical outcomes with low failure [8]. Complications of patellar fracture such as loss of reduction, nonunion, infection, post-traumatic arthritis, arthrofibrosis, symptomatic hardware may still exist [9,10]. For complication cases related to problematic hardware and

Peer review under responsibility of KeAi Communications Co., Ltd.
* Corresponding author. Department of Orthopaedics & Traumatology, The Chinese University of Hong Kong, Shatin, N.T., Hong Kong SAR, China.
E-mail address: lingqin@cuhk.edu.hk (L. Qin).

https://doi.org/10.1016/j.bioactmat.2021.03.044
Received 16 August 2020; Received in revised form 29 March 2021; Accepted 29 March 2021

implant irritation, a second surgery will be necessary to remove such implants [8,9]. The quality of life and pain outcomes of patients also improved significantly after removal of the implants [11]. Therefore, finding a material that is biodegradable in the body and enhances the healing of the fracture would be the most ideal.

Magnesium (Mg) is a biodegradable metal that has comparable elastic moduli and compressive yield strength to that of natural bone. These unique mechanical properties of Mg reduce stress shielding during load transfer after implantation of Mg implant [12]. Since Mg is biodegradable, the implant removal surgery could often be avoided. Mg implant had demonstrated osteogenic and angiogenic effects to healing bone [13–15]. Our previous study showed that implantation of Mg-based intramedullary nail for fracture fixation enhanced healing in closed fracture model in rats [14,16]. The osteopromotive property of Mg implant and its comparable mechanical properties to bone would make Mg an innovative and attractive fixation material to enhance patellar fracture repair. In the clinical practice for patellar fracture repair and rehabilitation, the patient's knee would be immobilized or a knee brace would be used for the first six weeks post-operation [17]. Therefore, the ideal material for making fixation pin will need to maintain sufficient mechanical strength during the first 6 weeks post-operation. We hypothesized that fixation of the patellar fracture with Mg pins and the degradation of the Mg pins after implantation would enhance fracture healing radiologically, mechanically, and histologically.

2. Methods

2.1. Transverse patellar fracture model in rabbits

Forty-eight 18-week-old female New Zealand White rabbits were obtained from the Laboratory Animal Service Center of the Chinese University of Hong Kong. Patellar fracture model was performed according to our established protocol [18,19]. Experimental procedures were approved by the Animal Experimentation Ethics Committee in the Chinese University of Hong Kong (Ref. No. 15/005/MIS). Briefly, a transverse osteotomy was performed between the proximal two-thirds and distal one-third of the patella by using an oscillating saw (Synthes; Mathys AG, Bettlach, Switzerland). A tunnel (ø 1.1 mm) was drilled longitudinally through the two bone fragments. A fixation pin (ø 1.0 mm; stainless-steel or pure Mg) was inserted into the tunnel. Mg pins used in this experiment (ø 1.0 mm, 99.99%) were purchased from Handan Longhai Special Metals, Ltd, China. The Mg pin was first extruded at a diameter about 3 mm and then cold drawn to a diameter of 1.0 mm. We have performed initial three-point bending mechanical test on these pure Mg pins that showed the failure load of 16.2 N and stiffness of 44.39 N/mm, respectively. A stainless steel cerclage wire (ø 0.6 mm; Synthes) was threaded through the ends of the K-wire to form a longitudinal "figure-of-eight" tension band at the anterior side of the patella (Fig. 1). This tension band wire was used to reduce and stabilize the whole construct and prevent the displacement of the two bone fragments. Figure-of-eight tension band wire was used because it provides higher stability than a circular wire [20]. Cast immobilization of the operated knee was applied on the operated knee for six weeks to prevent excess movement of the knee and mimic the clinical situation. Buprenorphine (0.03 mg/kg intramuscularly; Temgesic, Schering-Plough, Kenilworth, New Jersey) was injected 15 min before the operation and then daily for three days after the operation. The rabbits were allowed free cage activities and food access throughout the experiment.

The rabbits were euthanized at the end of week 8 or 12 after transverse osteotomy with an intravenous injection of an overdose of sodium pentobarbital. Two fluorochromes, calcein green (10 mg/kg; Sigma, Deisenhofen, Germany) and xylenol orange (90 mg/kg; Sigma), were injected subcutaneously at 2 and 1 week before euthanasia, respectively, for histological measurement of the rate of the new bone formation. The figure-of-8 tension band wire was removed and the quadriceps-patella-patellar tendon-tibia (QPPTT) complex of the operated knee was harvested. The QPPTT samples were then wrapped in gauze with saline, sealed in a freezer bag, and stored in a −80 °C freezer for further assessments.

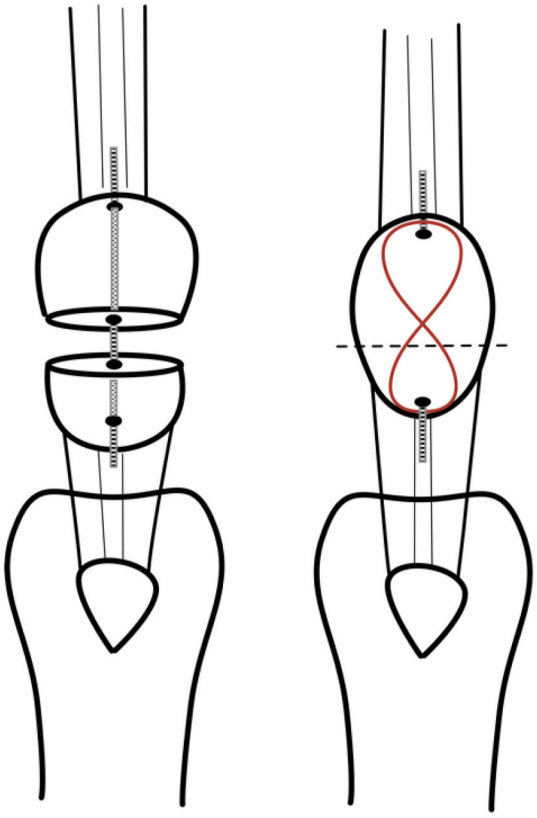

Fig. 1. Transverse patellar fracture model in rabbits was established according to our published protocol [18,19]. A: Transverse osteotomy was performed between the proximal two-thirds and distal one-third of the patella. A tunnel (ø 1.1 mm) was drilled longitudinally through the two bone fragments. A fixation pin (ø 1.0 mm; stainless steel or Mg) was inserted into the tunnel. A "figure-of-eight" tension band wire (ø 0.6 mm stainless steel wire; Synthes) was used to reduce and stabilize the whole construct, and to prevent displacement of the two bone fragments.

2.2. Radiological analysis

One of the complications of surgical repair for patellar fracture is the loss of fixation and reduction which would lead to displacement of the bone fragments. In the current experiment, failure of the implants would be one of the causes for the displacement of bone fragments. Since the Mg pins have a similar density on radiological images, the fracture gap cannot be identified. Therefore, the displacement of the two patellar bone fragments was estimated by measuring the total length of the patella at different time points. Briefly, the lateral radiological images were taken using a digital radiography system (UltraFocusDXA, Faxitron, Arizona US) at week 0, 4, 8, and 12 to monitor the healing progress of the patella fracture. Two experienced researchers, who were blinded from the time point and groupings of the samples, measured the total length of the repaired patella, from the base of the patella to the apex, at different time points.

2.3. Microarchitectural analysis and assessments of the degradation rate of Mg pins

Microarchitecture of the repaired patella was evaluated using a high-

resolution microCT (μCT-40; Scanco Medical, Brüttisellen, Switzerland) according to our established protocol [16]. The metal tension band wire, suture material, all periarticular connective soft tissues, and soft tissues around the knee were removed. The QPPTT was placed in the sample holder with their long axes in the vertical position. Samples were scanned in air instead of submerging in saline or ethanol during the scan. To prevent the sample from drying during the scanning, a piece of saline-soaked gauze was used to wrap around the entire sample. The whole PPT complex was scanned at an isotropic resolution of 20 μm^3. The beam energy was 70 kV, current intensity was 114 μA, and the integration time was 200 msec. The imaging data was then convoluted with a 3D Gaussian filter with a width and support equal to 1.2 and 2, respectively. Bone was segmented from the marrow and soft tissue for subsequent analysis using a global threshold, which was set to equal 165. Values equal to or greater than the threshold were used for representing bone tissue, while values below the threshold represented bone marrow and soft tissue [16,21]. Bone volume (BV), bone volume density (BV Density), tissue volume (TV), and the ratio of bone volume to tissue volume (BV/TV) were measured and evaluated. The volume of the Mg pins was measured with microCT to assess degradation rate of the pins.

2.4. Tensile testing of the repaired patella

The tensile strength was mechanically evaluated as the end point assessment of quality of the healing of the transverse patellar fracture. The QPPTT complex was thawed overnight at 4 °C. The QPPTT complex was mounted onto a custom-made fixator [16]. The QPPTT complex was mounted on a custom-made tensile testing jig (Supplementary Fig. 1), which consisted of an upper clamp and a lower clamp to fix the distal quadriceps plus the proximal patella and the proximal tibia, respectively. The distal quadriceps, its tendon, and the proximal patella were clamped directly in line with the axis of loading. A uniaxial mechanical testing machine (H25K–S, Hounsfield Test Equipment Ltd, Surrey, UK) with a 2.5 kN load cell was used, and a constant tensile load of 1 N was applied to the QPPTT complex. The thickness and width of the fracture site was measured with a fine calliper, and the cross-sectional area of the repaired patella was calculated. This value was used to normalize the tensile force (failure load) for calculating tensile strength [16]. Before the commencement of the tensile test, saline was applied to the QPPTT complex to keep the tissue moist and to prevent dehydration of the tissue. A load cell of 2.5 kN was used for recording tensile loading at a testing speed of 100 mm/min up to the failure of the QPPTT complex. The force-displacement curve of the tensile test was generated and failure load, ultimate strength, energy-to-failure, and stiffness were calculated.

2.5. Histological assessments

Histological sections of the repaired patella were stained according to our established protocols [16]. The tibia and distal quadriceps muscle were removed from the QPPTT complex to obtain the PPT complex for fixation in 4% paraformaldehyde solution and then cut into halves along its mid-sagittal plane using a thin blade saw. One half of the sample was used for decalcified histology while another half was used for undecalcified histology. For decalcified histology, the PPT complex were decalcified with EDTA and embedded in paraffin according to our established protocol [22,23]. Serial 5 μm thin sections from the mid-sagittal plane of each specimen were cut with a microtome. The sections were then stained with hematoxylin and eosin (H&E) or toluidine blue with fast green counter stain for general histological evaluation and assessment of the proteoglycan content of fracture site, respectively.

For undecalcified histology, the PPT complex was dehydrated in ethanol (70%, 95%, and 100%) and xylene. Then the sample was embedded in methylmethacrylate (MMA) according to an established protocol [23,24]. The embedded samples were sectioned sagittally (200 μm thick) using a diamond band-cutting machine (EXAKT Advanced Technologies GmbH, Norderstedt, Germany). The sections were then grinded and polished to 100 μm thick for imaging analysis under a fluorescence microscopy (Leica DM5500 B, Leica Cambridge Ltd, United Kingdom). The dynamics of osteogenesis, mineralization of new bone and its remodelling were investigated. Bone that was actively undergoing remodelling was labelled with the fluorochromes and was visualized and measured using L5 (calcein green only) and CY5 (xylenol orange only) filters. The mineral apposition rate was calculated by measuring the distance between the two fluorochrome labels and then divided this distance by the number of days separated between the injections, which was 7 days in the current experimental design.

2.6. Material properties of the new formed bone

Micro-indentation was performed on the sections of paraformaldehyde-fixed tissues at regenerated bone tissue according to the procedure outlined by the International Organization for Standardization (ISO 6507). The standard procedure, which was developed previously for testing the Vickers hardness (HV) of metal, was adopted for testing on anisotropic bone sections embedded in MMA in our early study [23,25]. Briefly, the surface of each section was polished before the indentation testing so the indentation marks were identifiable and measurable under the micro-indentation system. Individual section was placed under the microscope of the micro-indentation testing system (Dynamic Ultra Micro Hardness Tester, DUH-211 S, Shimadzu Corporation, Tokyo Japan) and region of interest (ROI) was identified. The Vickers diamond pyramidal indenter compressed at 25 g compression load onto the ROI for a dwell time of 10s. An indentation mark was formed on the ROI. The diagonal length of the indentation mark was measured and HV is calculated by the built-in software of the micro-indentor. The elastic modulus of the bone matrix was calculated from the unloading section of the force-displacement curve. Average HV and elastic modulus of regenerated bone matrix were calculated for statistical analysis.

2.7. Statistical analysis

All measurements were expressed as mean ± standard deviation (SD). All analysis was performed using SPSS 22.0 for Windows. Two-way Analysis of Variance (Two-way ANOVA) with Bonferroni post hoc test was used to detect differences between Mg pin group and the control group at the two time points. Statistical significance was set at $p < 0.05$.

3. Results

3.1. Radiological analysis

Length of the repaired patella measured on lateral radiological images at different time points. The length of the patella is used to estimate the stability of the repair construct with different metallic pins (Stainless steel, as the control, and Mg pin). Mg group showed comparable patella length to the control group at week 8 and 12 (Fig. 2, $p > 0.05$, $n = 8$).

3.2. Microarchitectural analysis

At week 8 and 12, the Control group and Mg group showed enlarged patella when compared to the normal patella. The new bone was formed at the lateral side of the patella for both the Control group and Mg group (Fig. 3). At week 8, the fracture gap was still visible for the control group and the Mg group. Mg group showed 12% higher in the ratio of bone volume to tissue volume (BV/TV) than the control group (Mg: 0.780 ± 0.09, Control: 0.694 ± 0.044; $p < 0.05$, Fig. 3). At week 12, the two bone fragments had been bridged and the fracture gap was not visible for both group (Fig. 3). Bone volume (BV) and Tissue volume (TV) of the patella

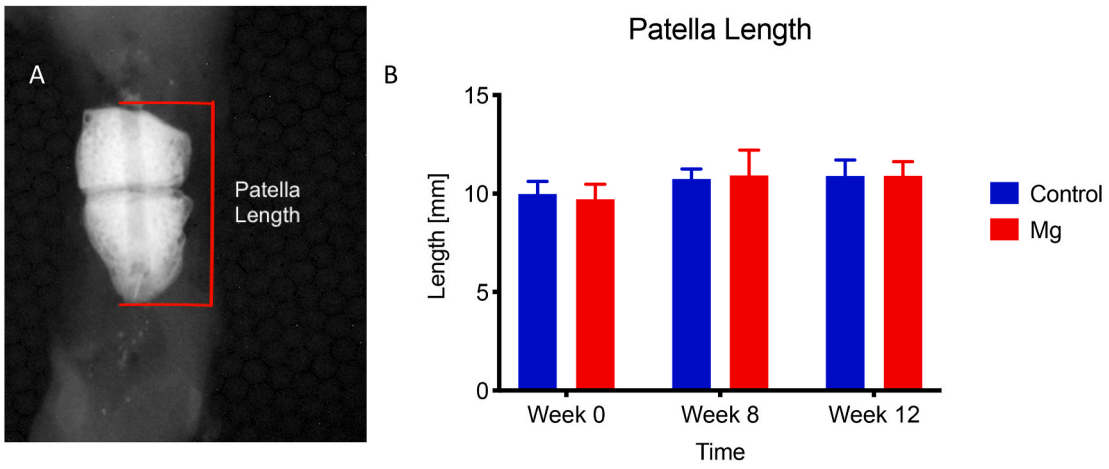

Fig. 2. Length of the repaired patella measured on lateral radiological images at week 0, 4, 8, and 12. The length of the patella was used to estimate the stability of the repair construct with different metallic pins (Stainless steel as the control, and Mg pin). A: The length of the patella was measured at the proximal pole of the patella to the distal pole. B: Mg group showed comparable patella length to the Control at week 0, 4, 8, and 12, without statistical significance at all time points ($p > 0.05$, $n = 8$).

in Mg group at week 12 was 38.4% ($p < 0.05$) and 22.7% ($p > 0.05$) higher than that of Control group, respectively. However, no significant difference was detected ($p > 0.05$) with respect to ratio of bone volume to tissue volume (BV/TV), TV density, and BV density between the Control group and Mg group at week 12.

3.3. Mechanical testing

Tensile testing was performed to measure the mechanical properties of the repaired patella, including failure load, stiffness, ultimate strength, and energy-to-failure. At week 8, the failure load and stiffness of the Mg group was 66.9% and 104% higher than that of the control group ($p < 0.05$), respectively (Fig. 4). At week 12, the ultimate strength of the Mg group was 60.8% higher than that of the control group ($p < 0.05$). The failure load and stiffness of the Mg group were also higher than that of the Control group (14.4% and 25.1% respectively) but no statistical significance was detected.

Hardness and modulus of elasticity of the newly formed bone at the fracture was measured using the undecalcified sections (Fig. 5). Mg group showed 49.9% ($p < 0.05$) higher Vickers hardness than the control group at week 8. At week 12, Mg group showed 31% ($p < 0.05$) higher modulus of elasticity than the Control group (Fig. 5).

3.4. Histological analysis

Histological analysis showed that patellar fracture repair was characterized with endochondro-ossification and progressive remodelling at the healing interface overtime (Figs. 6 and 7). There was significant more new bone formation at the fracture site in the Mg group than the Control group at week 8 and 12. At week 8, the histological images show that there were new bone formation and cartilaginous tissue at the fracture for both the control group and the Mg group (Figs. 6 and 7). The new bone formed in both groups at week 8 was woven bone. At week 12, the new bone remodelled to laminar bone for the Mg group but the new bone of the control group still kept the morphology of woven bone (Fig. 6).

For the dynamic histomorphometric analysis, the Mg group showed a higher mineral apposition rate than the control at week 12 while there was no significant difference between the two groups at week 8 (Fig. 8).

3.5. Degradation of Mg pins in vivo

The degradation rate of the Mg pins at baseline, week 8, and week 12 were measured with μCT. The volumes of the Mg pin were 6.184 ± 0.76 mm^3 and 3.606 ± 0.65 mm^3 at week 8 and 12, respectively (Fig. 9A). The percentage degraded in volume of Mg pins equaled to 22.44% and 54.8% at week 8 and 12 respectively (Fig. 9B).

4. Discussion

The current study investigated the effect of using a biodegradable Mg pin and figure-of-eight tension band for fixation of patellar fracture using an osteotomy model of patella in rabbits. Mechanical testing, microarchitectural analysis, and histological assessments confirmed our hypothesis that Mg pins and its degradation with implantation over time would enhance healing of patellar fracture radiologically, mechanically, and histologically. Our results demonstrated that fixation of patellar fracture using biodegradable Mg pin enhanced new bone formation, microarchitectural parameters, and mechanical properties of the repaired patella compared to the Control using stainless steel pin.

Reduction of the patellar fracture with Mg pin and stainless steel tension band wire enhanced healing of the fracture with respect to mechanical properties, new bone formed, and histological analysis. Patellar fracture repair was characterized with endochondro-ossification and progressive remodelling at the healing interface overtime. In the control group, there was more cartilaginous tissue at the healing interface at week 8 than week 12 post-operation. This suggested that these cartilaginous tissues were remodelled to bone tissue through endochondral ossification, a well-known mechanism in bone fracture healing. Our histological finding was comparable to the observation by Leung et al. [18]. Furthermore, at week 12, the Mg group showed minimal cartilaginous tissue at the fracture gap (Figs. 6 and 7), higher ultimate strength (Fig. 4), and higher modulus of elasticity (Fig. 7) as compared to the control group. These suggested that the newly formed bone at the fracture site of the patellae in the Mg group had higher material properties than that of the control at week 12. This suggested that Mg pin accelerated the healing of patellar fracture by enhancing or accelerating the remodelling of the tissues at the healing interface.

Mg ions that were released during the degradation of the Mg pin might contribute to the enhanced fracture repair. In our published study, Mg ions, released from an innovative intramedullary nail, enhanced fracture healing by improving osteogenesis via stimulation of local release of calcitonin-gene related peptide (CGRP) from periosteum [14]. Periosteum contains many sensory nerve endings which release CGRP and demonstrates the beneficial effect of Mg ions. CGRP is a neuropeptide and involves in the healing and remodelling of bone [26–29]

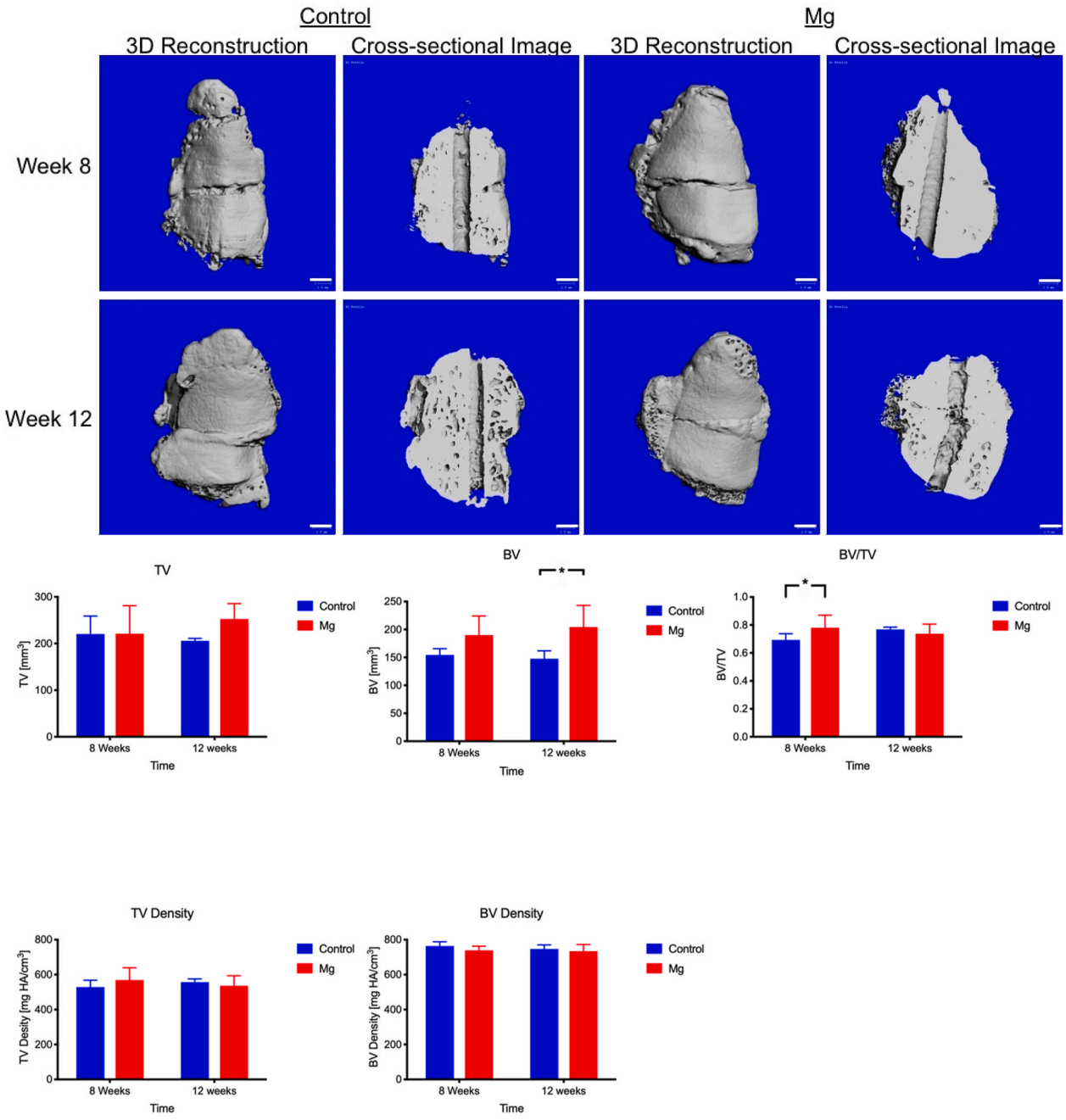

Fig. 3. Representative 3-dimensional and cross-sectional microCT images, and microarchitectural analysis of the healing patella of the Control group and Mg group at week 8 and week 12. A: Mg group showed more new bone formation than the Control group at week 8 and 12. B: At week 8, Mg group showed a significantly higher ratio of bone volume to tissue volume (BV/TV). At week 12, Mg group showed significantly greater bone volume (BV). There was no significant difference in TV density and BV density between the Control group and the Mg group at all time points. *: $p < 0.05$, $n = 8$, Scale bar: 1 mm.

and tendon [30,31]. However, the patella does not have periosteum and the repair of the patellar fracture did not proceed with a formation of a periosteum callus (Figs. 6 and 7) [18]. One of the explanations for this enhancement is that there are intraosseous innervation in the patella [32] and sensory nerves in the patellar tendon [33]. These nerves may be stimulated by the Mg ions and release the CGRP neuropeptide to enhancing the healing of patellar fracture. Mg ions were also shown to enhance the osteogenic activity of bone marrow stromal cells via upregulation of collagen type X and vascular endothelial growth factor (VEGF) [34]. VEGF is an essential factor that is important for the formation of type H vessels, which may regulate bone homeostasis [35].

Degradation of our pure Mg pin in the patella was faster than the degradation rates of pure Mg implants published by others. In the current study, the degradation rate of our Mg pin was a decrease in volume of the pin by 22.4% at week 8 and 54.8% at week 12. Huang et al. implanted high purity Mg screw for fixation of femoral neck fracture in goats and they reported that the degradation rate was decrease in volume of the pin by 10% at week 4 and 38.8% at week 12 [36]. Zhao et al. implanted pure Mg (99.99%) screw for fixation of a vascularized bone graft to treat osteonecrosis of femoral head in humans [36]. They reported that the average reduction percentage of Mg screw diameter was 3.7%, 9.3%, 13.7% and 25.2% at 1, 3, 6, and 12 months, postoperatively [36]. Wang et al. implanted high purity Mg interference screw for anterior cruciate ligament reconstruction in rabbits and reported that the degradation rate of the interference screw was decrease in volume of the screw by 10% after 16 weeks post-operation [36]. One

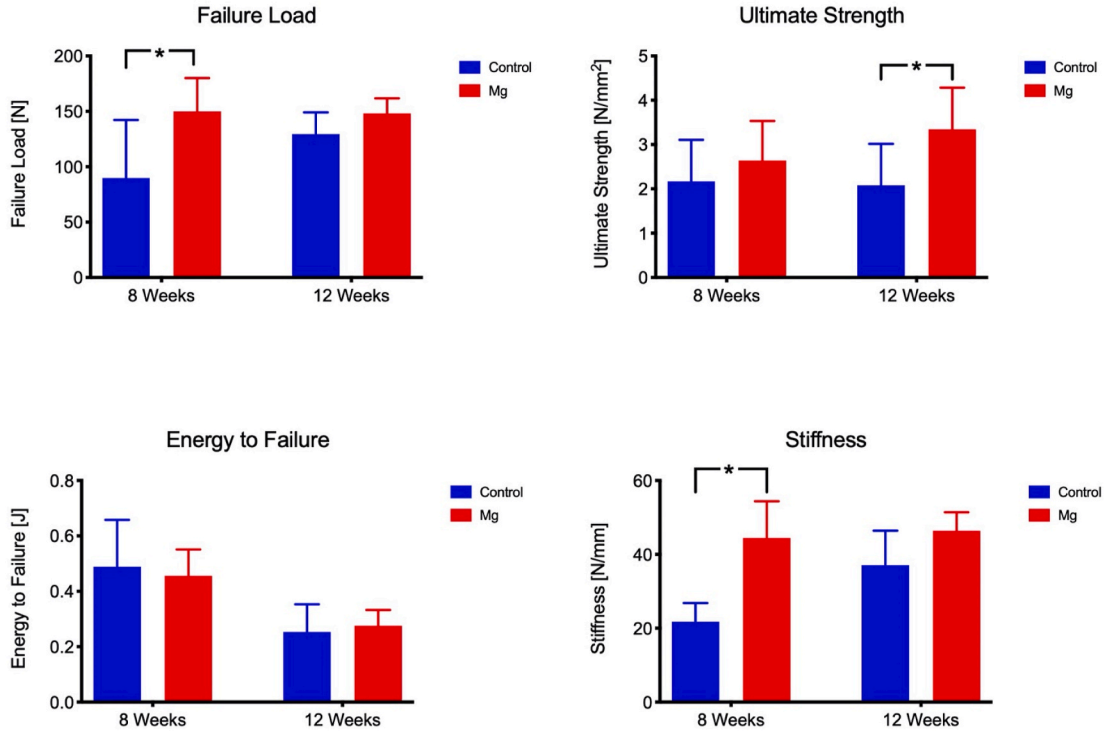

Fig. 4. Tensile testing for mechanical properties of the repair construct. *: $p < 0.05$. Mg group had higher failure load than the control at week 8. At week 12, both the ultimate strength and the stiffness of the Mg group were higher than the control group.

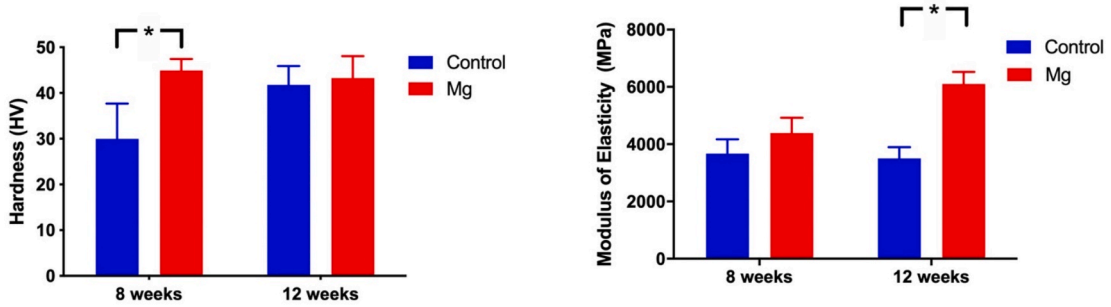

Fig. 5. Hardness and elastic modulus of the newly formed bone at the fracture or osteotomy site. Mg group showed higher Vickers hardness (HV) than the control group at week 8. At week 12, Mg group showed higher modulus of elasticity than the Control group. *: $p < 0.05$.

of the reasons that the current study demonstrated faster degradation of the Mg implant was the presence of implants that are made of another metal, which is the stainless steel wire for the tension band. The presence of other metals can cause electrolytic corrosion of Mg [37]. This suggested that a higher quantity of Mg than needed for the expected time period should be used for better and safer fixation. One of the approaches that prevent rapid degradation of the Mg implant would be by applying coatings [38,39], surface treatments [40,41], and alloying [42,43] to decrease the degradation rate of the Mg implants. Therefore, these methods are necessary for Mg implants when other metallic implants are in close proximity to the Mg implant to prevent early unexpected failure of the Mg implant.

Mechanical strength of Mg pin developed in the current study was sufficient for reduction of patellar fracture with the figure-of-eight tension band in rabbits. However, there are a few limitations in application of Mg metals in orthopaedics such as the rapid degradation of the metal which may further weaken the mechanical properties of the Mg implant. We have recognized this challenge and designed innovative hybrid fixation systems recently [38,44] for avoiding such problem. In the current study we used pure Mg K-wire with stainless steel wire for figure-of eight protection band wire. This allowed sufficient fixation during the early phase of the fracture healing to bridge the two patellar fragments. Furthermore, the Mg pin that we used in the current study has a high purity of 99.99% that showed slower degradation than those of less pure Mg pin (purity less than 99.99%, such as 99.9% [12]. By applying the high purity Mg pin and developing hybrid fixation method, we demonstrated in the current study that it was feasible to use degradable Mg pin for effective patellar fracture fixation and healing enhancement. One of the early complications for the surgical repair of patellar fractures is the loss of reduction or fixation of the bone fragments. Smith et al. reported that there was a 22% of fracture treated with tension band wiring and early motion displaced greater than or equal to 2 mm during the early postoperative period [10]. From our current study, although a cast was placed on the operated knee to reduce the motion of the knee joint, the rabbit could still move around the cage and some movement of the operated knee was also observed. Since there was no fracture gap at week 12, and no significant difference of the patella length between Mg group and the control group at week 8 and 12 (Fig. 2B), the Mg pin with the stainless steel cerclage wire were sufficient for reducing the patellar fracture while allowing some early movement of the operated knee.

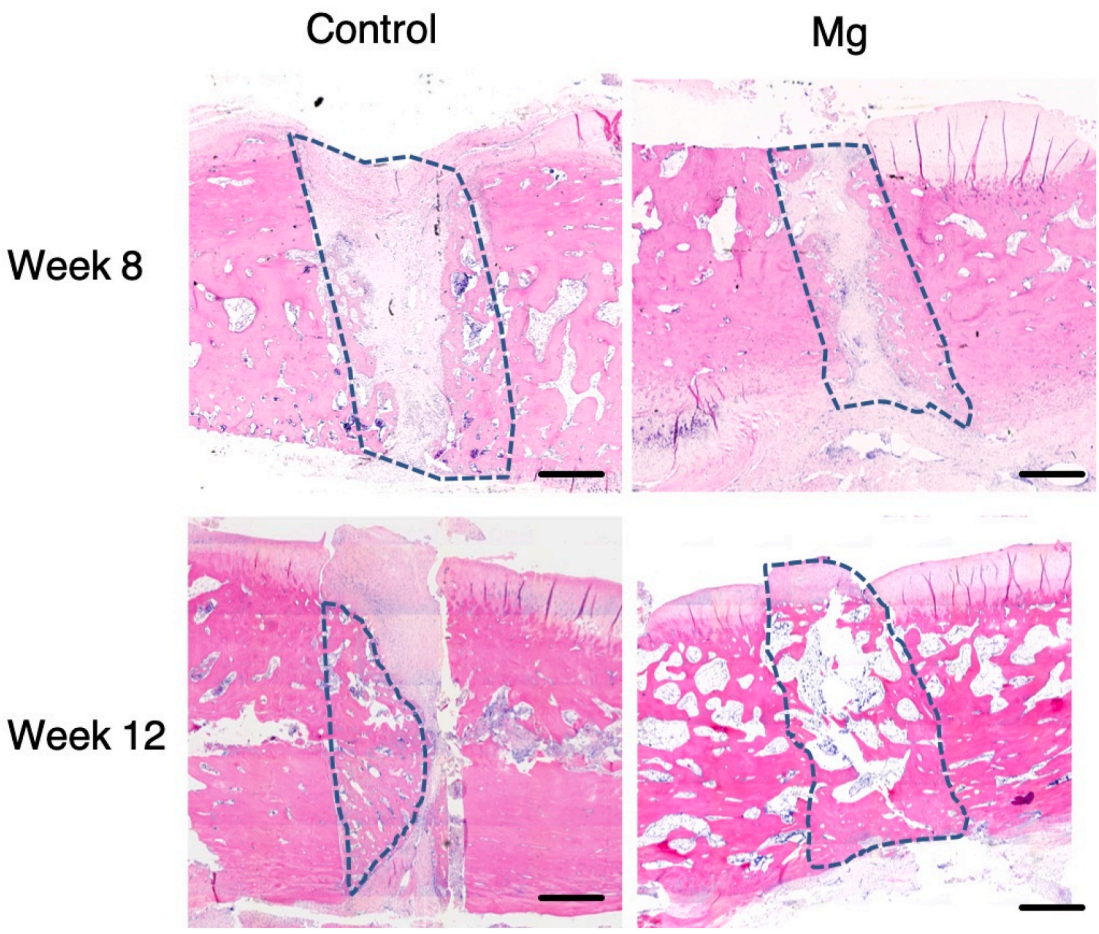

Fig. 6. Representative hematoxylin and eosin-stained sections of the healing patella at the fracture site of the Control group and Mg group at week 8 and week 12. Mg group showed more new bone formation than the control group at week 8. At week 12, the Mg group showed more new bone formation that bridged the bone fragments than that of the Control group. The dotted line outlined the area of the newly formed bone. Magnification: 50 × . Scale bar: 1 mm.

The high purity Mg pins that were used in the current study have a purity of 99.99% (4 N), which is higher than those available ones which have a purity of 99.9% (3 N). These high purity pins were developed to avoid concerns and potential health risks of alloying elements in patients [12] and accelerated degradation due to impurities of Mg [45]. High purity 99.99% Mg pins showed a slower degradation rate than those with less purity, e.g. purity of 99.9% Mg pin [12,45]. In addition to pins, these high purity Mg metal has been fabricated into screws and have been used to fix autologous vascularized bony flaps to treat avascular necrosis of the femoral head in patients in our previous clinical study [46]. However, Mg implants alone are not suitable at weight-bearing site due to rather fast degradation of Mg implants and limited mechanical properties (e.g. durability and strength). We have developed hybrid fixation systems for avoiding such potential clinical risks [38,44]. In the current study, the mechanical support of the whole construct is also contributed by the high purity Mg pin and stainless-steel tension band wire. This allowed sufficient fixation during the early phase of the fracture healing to bridge the two patellar fragments. The combined usage of Mg implant and permeant implant made the application of Mg-based implant feasible at weight-bearing site. Tian *et al.* proposed a hybrid compression plate-screw design which one of the screws near the fracture site is made of pure Mg while the other screws and the compression plate were made of titanium [44].

The absolute values of the tissue density measurements of the present study may not be comparable to other published data as our samples were scanned in air [47]. The density measurements that were generated from our samples may not be accurately reflect their absolute density value due to the automatic calibration and scanning assumptions of the scanner, which the scanning of the samples is assumed to be performed in a liquid medium. In the current experiment, we compared the measurements of different samples within the same experiment that were scanned under the same conditions. This suggests that although the absolute tissue mineral density may be different from the actual values, their relative values would still be comparable among samples for statistical analysis.

For our future studies, the next logical improvement to the current proof-of-concept approach is to replace the stainless-steel cerclage wire by a biodegradable Mg-based wire. In the current study, a non-biodegradable stainless-steel cerclage wire was used to prevent the displacement of the bone fragments during movement of the rabbits. This cerclage wire will still need to be surgically removed when the fracture has healed completely. By using a Mg-based cerclage wire, this wire will be slowly degraded without performing implant removal surgery. The Mg alloy cerclage wire would need to have sufficient strength to withstand the tensile forces generated in the figure-of-eight loop [2]. The feasibility of using Mg alloy cerclage wire shall be further explored in our clinical settings.

5. Conclusion

In the fixation of transverse patellar fracture with tension band wire, Mg pins enhanced new bone formation and mechanical properties of the repaired patella, with respect to radiological, histological, and mechanical assessments, compared to the Control group, which used stainless steel wire. The results formed the foundation for designing clinical trials on the application of biodegradable Mg implants and

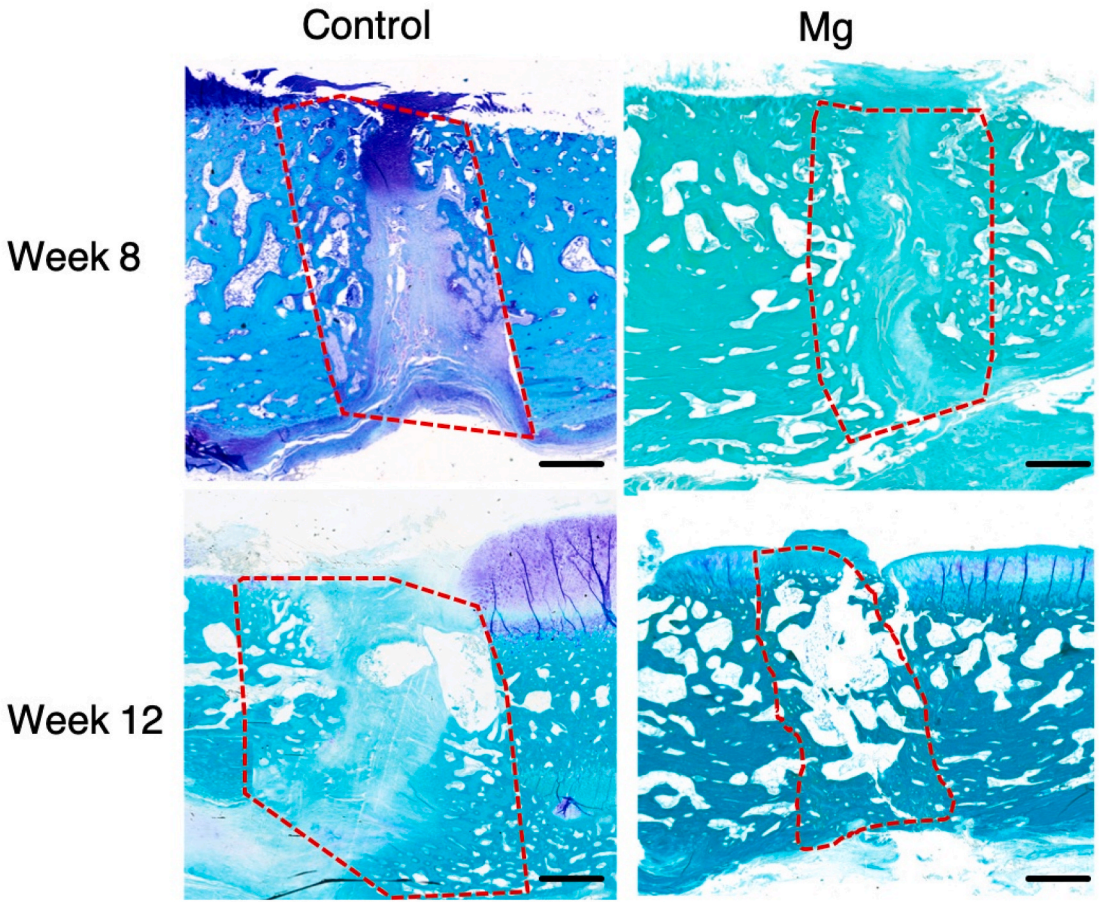

Fig. 7. Representative toluidine blue-stained sections of the healing patella at the fracture site of the Control group and Mg group at week 8 and week 12, post-operatively. Mg group showed more new bone formation than the control group at week 8. Both groups showed that there was cartilaginous tissue at the fracture site. At week 12, Mg group showed more new bone formation and bridging of the bone fragments than the Control group. Both groups showed that the cartilaginous tissue was calcified and remodelled towards lamellar bone. The dotted line outlined the area of the newly formed bone. Magnification: 50 × . Scale bar: 1 mm.

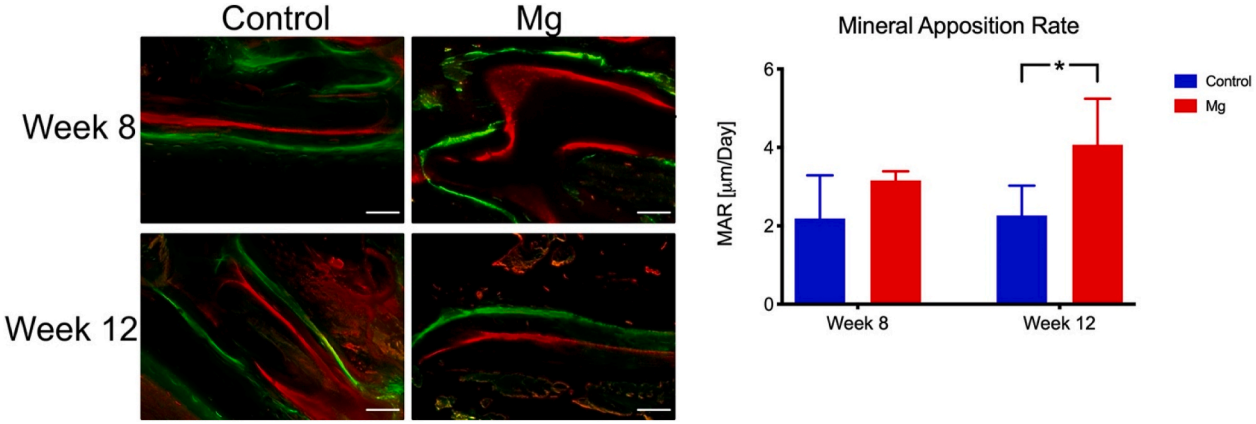

Fig. 8. New bone formation at the fracture site of the patella. A: Representative fluorochrome images of the Control group and the Mg group. The dynamic process of the bone formation at the fracture is showed. B. The higher bone mineral apposition rate of the Mg group was higher than the Control group at week 12. *: $p < 0.05$, $n = 5$, Scale bar = 50 μm.

provide a suggestion on the joint application of other metallic implants with Mg implants. The results might also be applicable to other problematic fractures which K-wire and tension band wire fixation method is commonly used.

CRediT authorship contribution statement

Dick Ho Kiu Chow: Conceptualization, Methodology, Investigation, Formal analysis, Writing – original draft. **Jiali Wang:** Conceptualization, Methodology. **Peng Wan:** Investigation, Methodology, Formal analysis. **Lizhen Zheng:** Investigation, Formal analysis. **Michael Tim Yun Ong:** Writing – review & editing. **Le Huang:** Investigation, Formal

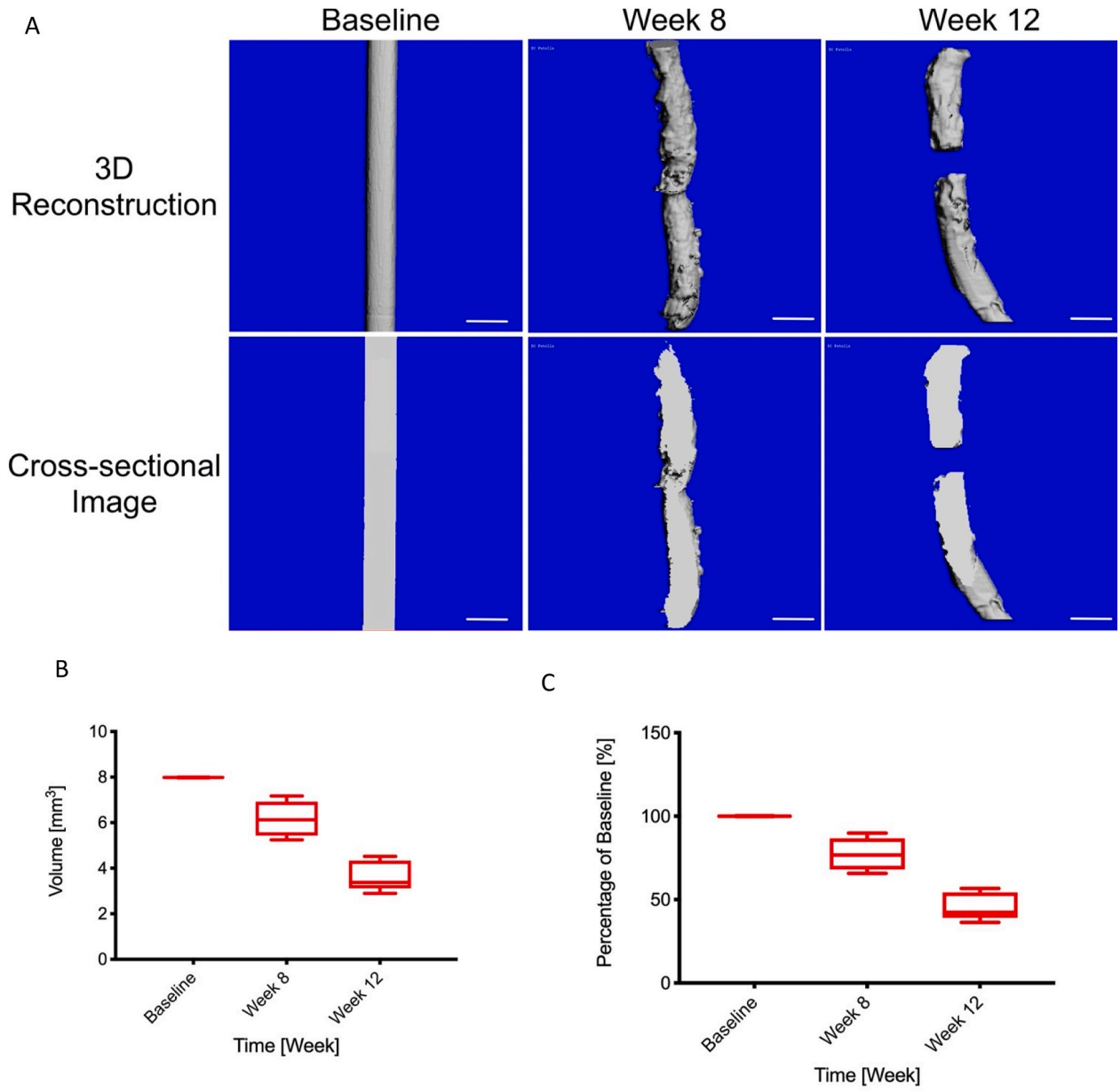

Fig. 9. The volume of the Mg pin measured by μCT at different time point. A: The Three-dimensional reconstruction and cross-sectional images of the Mg pins scanned by microCT at baseline, week 8, and week 12. B: The volumes of the Mg pin were 6.184 ± 0.76 mm^3 and 3.606 ± 0.65 mm^3 at week 8 and 12, respectively. C: The percentage remaining in the volume of Mg pins equaled to 22.44% and 54.8% at week 8 and 12 respectively.

analysis. **Wenxue Tong:** Investigation, Formal analysis. **Lili Tan:** Resources, Supervision, Formal analysis. **Ke Yang:** Funding acquisition, Resources, Supervision. **Ling Qin:** Funding acquisition, Resources, Supervision, Writing – review & editing.

Declaration of competing interest

The authors declare that they have no known competing financial interests or personal relationships that could have appeared to influence the work reported in this paper.

Acknowledgement

This work was supported by Chinese Academy of Sciences-Croucher Funding Scheme for Joint Laboratory (CAS14303), and partially supported by Theme-based Research Scheme (Ref No. T13-402/17-N) and Collaborative Research Fund (Ref No. C4026-17W) from the University Grant Committee of the Hong Kong Special Administrative Region, China.

Appendix A. Supplementary data

Supplementary data to this article can be found online at https://doi.org/10.1016/j.bioactmat.2021.03.044.

References

[1] A. Bostrom, Fracture of the patella. A study of 422 patellar fractures, Acta Orthop. Scand. Suppl. 143 (1972) 1–80.
[2] T.P. Rüedi, W.M. Murphy, AO Principles of Fracture Management, Thieme; AO Pub., Stuttgart ; New York Davos Platz, Switzerland, 2000.
[3] J.D. Trojan, J.A. Treloar, C.M. Smith, M.J. Kraeutler, M.K. Mulcahey, Epidemiological patterns of patellofemoral injuries in collegiate athletes in the United States from 2009 to 2014, Orthop J Sports Med 7 (4) (2019), 2325967119840712.

[4] S.E. Byun, J.A. Sim, Y.B. Joo, J.W. Kim, W. Choi, Y.G. Na, O.J. Shon, Changes in patellar fracture characteristics: a multicenter retrospective analysis of 1596 patellar fracture cases between 2003 and 2017, Injury 50 (12) (2019) 2287–2291.

[5] J. Nummi, Fracture of the patella. A clinical study of 707 patellar fractures, Ann. Chir. Gynaecol Fenn. Suppl. 179 (1971) 1–85.

[6] L. Camarda, S. Morello, F. Balistreri, A. D'Arienzo, M. D'Arienzo, Non-metallic implant for patellar fracture fixation: a systematic review, Injury 47 (8) (2016) 1613–1617.

[7] P.A. Lotke, M.L. Ecker, Transverse fractures of the patella, Clin. Orthop. Relat. Res. 158 (1981) 180–184.

[8] K.L. Hsu, W.L. Chang, C.Y. Yang, M.L. Yeh, C.W. Chang, Factors affecting the outcomes of modified tension band wiring techniques in transverse patellar fractures, Injury 48 (12) (2017) 2800–2806.

[9] J. Petrie, A. Sassoon, J. Langford, Complications of patellar fracture repair: treatment and results, J. Knee Surg. 26 (5) (2013) 309–312.

[10] S.T. Smith, K.E. Cramer, D.E. Karges, J.T. Watson, B.R. Moed, Early complications in the operative treatment of patella fractures, J. Orthop. Trauma 11 (3) (1997) 183–187.

[11] A. Greenberg, A. Kadar, M. Drexler, Z.T. Sharfman, O. Chechik, E.L. Steinberg, N. Snir, Functional outcomes after removal of hardware in patellar fracture: are we helping our patients? Arch. Orthop. Trauma. Surg. 138 (3) (2018) 325–330.

[12] J.L. Wang, J.K. Xu, C. Hopkins, D.H. Chow, L. Qin, Biodegradable magnesium-based implants in orthopedics-a general review and perspectives, Adv. Sci. 7 (8) (2020) 1902443.

[13] X. Lin, J. Ge, D. Wei, C. Liu, L. Tan, H. Yang, K. Yang, H. Zhou, B. Li, Z.P. Luo, L. Yang, Surface degradation-enabled osseointegrative, angiogenic and antiinfective properties of magnesium-modified acrylic bone cement, J Orthop Translat 17 (2019) 121–132.

[14] Y. Zhang, J. Xu, Y.C. Ruan, M.K. Yu, M. O'Laughlin, H. Wise, D. Chen, L. Tian, D. Shi, J. Wang, S. Chen, J.Q. Feng, D.H. Chow, X. Xie, L. Zheng, L. Huang, S. Huang, K. Leung, N. Lu, L. Zhao, H. Li, D. Zhao, X. Guo, K. Chan, F. Witte, H. C. Chan, Y. Zheng, L. Qin, Implant-derived magnesium induces local neuronal production of CGRP to improve bone-fracture healing in rats, Nat. Med. 22 (10) (2016) 1160–1169.

[15] W. Yu, R. Li, J. Long, P. Chen, A. Hou, L. Li, X. Sun, G. Zheng, H. Meng, Y. Wang, A. Wang, X. Sui, Q. Guo, S. Tao, J. Peng, L. Qin, S. Lu, Y. Lai, Use of a three-dimensional printed polylactide-coglycolide/tricalcium phosphate composite scaffold incorporating magnesium powder to enhance bone defect repair in rabbits, J Orthop Translat 16 (2019) 62–70.

[16] D.H. Chow, P.K. Suen, L.H. Fu, W.H. Cheung, K.S. Leung, M.W. Wong, L. Qin, Extracorporeal shockwave therapy for treatment of delayed tendon-bone insertion healing in a rabbit model: a dose-response study, Am. J. Sports Med. 40 (12) (2012) 2862–2871.

[17] J.S. Melvin, S. Mehta, Patellar fractures in adults, J. Am. Acad. Orthop. Surg. 19 (4) (2011) 198–207.

[18] K.S. Leung, L. Qin, L.K. Fu, C.W. Chan, A comparative study of bone to bone repair and bone to tendon healing in patella-patellar tendon complex in rabbits, Clin. Biomech. 17 (8) (2002) 594–602.

[19] C.D. Newton, D.M. Nunamaker, Textbook of Small Animal Orthopaedics, Lippincott, Philadelphia, 1985.

[20] K.J. Koval, Y.H. Kim, Patella fractures. Evaluation and treatment, Am. J. Knee Surg. 10 (2) (1997) 101–108.

[21] D.H. Chow, K.S. Leung, L. Qin, A.H. Leung, W.H. Cheung, Low-magnitude high-frequency vibration (LMHFV) enhances bone remodeling in osteoporotic rat femoral fracture healing, J. Orthop. Res. 29 (5) (2011) 746–752.

[22] D.H. Chow, L. Zheng, L. Tian, K.S. Ho, L. Qin, X. Guo, Application of ultrasound accelerates the decalcification process of bone matrix without affecting histological and immunohistochemical analysis, J Orthop Translat 17 (2019) 112–120.

[23] D.H. Chow, P.K. Suen, L. Huang, W.H. Cheung, K.S. Leung, C. Ng, S.Q. Shi, M. W. Wong, L. Qin, Extracorporeal shockwave enhanced regeneration of fibrocartilage in a delayed tendon-bone insertion repair model, J. Orthop. Res. 32 (4) (2014) 507–514.

[24] K.S. Leung, A Practical Manual for Musculoskeletal Research, World Scientific, Singapore, 2008.

[25] L. Qin, P. Fok, H. Lu, S. Shi, Y. Leng, K. Leung, Low intensity pulsed ultrasound increases the matrix hardness of the healing tissues at bone-tendon insertion-a partial patellectomy model in rabbits, Clin. Biomech. 21 (4) (2006) 387–394.

[26] K. Irie, F. Hara-Irie, H. Ozawa, T. Yajima, Calcitonin gene-related peptide (CGRP)-containing nerve fibers in bone tissue and their involvement in bone remodeling, Microsc. Res. Tech. 58 (2) (2002) 85–90.

[27] S.J. Sample, Z. Hao, A.P. Wilson, P. Muir, Role of calcitonin gene-related peptide in bone repair after cyclic fatigue loading, PloS One 6 (6) (2011), e20386.

[28] S. Imai, Y. Matsusue, Neuronal regulation of bone metabolism and anabolism: calcitonin gene-related peptide-, substance P-, and tyrosine hydroxylase-containing nerves and the bone, Microsc. Res. Tech. 58 (2) (2002) 61–69.

[29] J. Mi, J. Xu, H. Yao, X. Li, W. Tong, Y. Li, B. Dai, X. He, D.H.K. Chow, G. Li, K. O. Lui, J. Zhao, L. Qin, Calcitonin gene-related peptide enhances distraction osteogenesis by increasing angiogenesis, Tissue Eng. Pt A. 27 (2021) 87–102, https://doi.org/10.1089/ten.tea.2020.0009.

[30] P.W. Ackermann, M. Ahmed, A. Kreicbergs, Early nerve regeneration after achilles tendon rupture–a prerequisite for healing? A study in the rat, J. Orthop. Res. 20 (4) (2002) 849–856.

[31] P.W. Ackermann, Neuronal regulation of tendon homoeostasis, Int. J. Exp. Pathol. 94 (4) (2013) 271–286.

[32] R.S. Barton, M.L. Ostrowski, T.D. Anderson, O.A. Ilahi, M.H. Heggeness, Intraosseous innervation of the human patella: a histologic study, Am. J. Sports Med. 35 (2) (2007) 307–311.

[33] G. Maralcan, I. Kuru, S. Issi, A.F. Esmer, I. Tekdemir, D. Evcik, The innervation of patella: anatomical and clinical study, Surg. Radiol. Anat. 27 (4) (2005) 331–335.

[34] S. Yoshizawa, A. Brown, A. Barchowsky, C. Sfeir, Magnesium ion stimulation of bone marrow stromal cells enhances osteogenic activity, simulating the effect of magnesium alloy degradation, Acta Biomater. 10 (6) (2014) 2834–2842.

[35] Y. Peng, S. Wu, Y. Li, J.L. Crane, Type H blood vessels in bone modeling and remodeling, Theranostics 10 (1) (2020) 426–436.

[36] S. Huang, B. Wang, X. Zhang, F. Lu, Z. Wang, S. Tian, D. Li, J. Yang, F. Cao, L. Cheng, Z. Gao, Y. Li, K. Qin, D. Zhao, High-purity weight-bearing magnesium screw: translational application in the healing of femoral neck fracture, Biomaterials 238 (2020) 119829.

[37] F. Witte, The history of biodegradable magnesium implants: a review, Acta Biomater. 6 (5) (2010) 1680–1692.

[38] L. Tian, Y. Sheng, L. Huang, D.H. Chow, W.H. Chau, N. Tang, T. Ngai, C. Wu, J. Lu, L. Qin, An innovative Mg/Ti hybrid fixation system developed for fracture fixation and healing enhancement at load-bearing skeletal site, Biomaterials 180 (2018) 173–183.

[39] S. Chen, P. Wan, B. Zhang, K. Yang, Y. Li, Facile fabrication of the zoledronate-incorporated coating on magnesium alloy for orthopaedic implants, J Orthop Translat 22 (2020) 2–6.

[40] X.D. Yan, M.C. Zhao, Y. Yang, L.L. Tan, Y.C. Zhao, D.F. Yin, K. Yang, A. Atrens, Improvement of biodegradable and antibacterial properties by solution treatment and micro-arc oxidation (MAO) of a magnesium alloy with a trace of copper, Corrosion Sci. 156 (2019) 125–138.

[41] M.M. Gawlik, B. Wiese, V. Desharnais, T. Ebel, R. Willumeit-Romer, The effect of surface treatments on the degradation of biomedical Mg alloys-a review paper, Materials 11 (12) (2018).

[42] K. Chen, X. Xie, H. Tang, H. Sun, L. Qin, Y. Zheng, X. Gu, Y. Fan, In vitro and in vivo degradation behavior of Mg-2Sr-Ca and Mg-2Sr-Zn alloys, Bioact Mater 5 (2) (2020) 275–285.

[43] M. Pogorielov, E. Husak, A. Solodivnik, S. Zhdanov, Magnesium-based biodegradable alloys: degradation, application, and alloying elements, Interv Med Appl Sci 9 (1) (2017) 27–38.

[44] L. Tian, N. Tang, T. Ngai, C. Wu, Y. Ruan, L. Huang, L. Qin, Hybrid fracture fixation systems developed for orthopaedic applications: a general review, J Orthop Translat 16 (2019) 1–13.

[45] B. Yang, F. Liu, B.-Y. Liu, Z.-M. Chang, L.-Y. Mao, J. Li, Z.-W. Shan, Producing High Purity Magnesium (99.99%) Directly by Pidgeon Process, Springer International Publishing, 2020, pp. 299–302. Cham %@ 978-3-030-36647-6.

[46] D.W. Zhao, S.B. Huang, F.Q. Lu, B.J. Wang, L. Yang, L. Qin, K. Yang, Y.D. Li, W. R. Li, W. Wang, S.M. Tian, X.Z. Zhang, W.B. Gao, Z.P. Wang, Y. Zhang, X.H. Xie, J. L. Wang, J.L. Li, Vascularized bone grafting fixed by biodegradable magnesium screw for treating osteonecrosis of the femoral head, Biomaterials 81 (2016) 84–92.

[47] M.L. Bouxsein, S.K. Boyd, B.A. Christiansen, R.E. Guldberg, K.J. Jepsen, R. Müller, Guidelines for assessment of bone microstructure in rodents using micro-computed tomography, J. Bone Miner. Res. 25 (7) (2010) 1468–1486.